Improved Variational Denoising of Flow Fields with Application to Phase-Contrast MRI Data

Emrah Bostan, *Student Member, IEEE*, Stamatios Lefkimmiatis, *Member, IEEE*, Orestis Vardoulis, *Student Member, IEEE*, Nikolaos Stergiopulos, and Michael Unser, *Fellow, IEEE*

***Abstract*—We propose a new variational framework for the problem of reconstructing flow fields from noisy measurements. The formalism is based on regularizers penalizing the singular values of the Jacobian of the field. Specifically, we rely on the nuclear norm. Our method is invariant with respect to fundamental transformations and can be efficiently solved. We conduct numerical experiments on several phantom data and report improved performance compared to existing vectorial extensions of total variation and curl-divergence regularizations. Finally, we apply our reconstruction method to an experimentally-acquired phase-contrast MRI recording for enhancing the data visualization.**

***Index Terms*—4D MRI, denoising, flow fields, flow MRI, Jacobian, PCMRI, phase-constrast MRI, regularization, Schatten norms, vector fields, vectorial total variation.**

I. Introduction

REGULARIZED reconstruction of flow data is becoming a prominent subject of research. This is partly due to the appearance of vector fields as the appropriate mathematical representation of objects of interest (for instance, the displacement field in motion estimation, or the deformation field for image registration). More importantly, recent progress in imaging technologies enables direct measurements of flows as vector quantities. The optical measurement technique known as the particle image velocimetry (PIV) provides instantaneous velocity vector measurements in fluid flows [1]. Another modality used in velocity field imaging is called the phase-contrast magnetic resonance imaging (PC MRI) in which we shall specifically be interested. PC MRI allows the acquisition of blood flow with a volumetric coverage in a time-resolved fashion [2]. Since measurement noise and imperfections are always present, it is of interest to develop methods that can remove these perturbations efficiently. Practically speaking, such algorithms are useful for data visualization and quantitative analysis.

Variational denoising algorithms have been investigated noticeably from two main perspectives. One approach is to impose certain physical attributes as the field measurements are fundamentally related to some physical phenomenon. Accordingly, curl and divergence operators are frequently used since they control the rotational and laminar characteristics, respectively. Combined with vector L_1-norms, these regularizers have been effectively used for denoising fields with discontinuities (occurring at interfaces between different fluids and object boundaries) [3]–[5] and overperformed their quadratic counterparts [6]–[8]. Another approach is based on modeling multi-channel data (for example, color and hyperspectral images) as vector-valued functions. Likewise, the design goal is to effectively couple the information coming from different channels as the discontinuities are preserved. Researchers have designed vectorial extensions of total variation (TV) regularization following its success for scalar fields [9]–[11].

In the present paper, we are interested in a reconstruction framework that is well-suited for flow fields with discontinuities. Our guiding principle is to regulate the vector-variations through the consideration of a local geometry. To that purpose, we follow our previous line of research [11] and employ a regularizer that penalizes the singular values of the Jacobian operator.

The main contributions of this work are: 1) The formulation of a regularization scheme that is appropriate for flow field denoising. The regularizer—termed as nuclear total variation (TVN)—penalizes the nuclear norm of the Jacobian evaluated at every spatial location of the flow. We show that this regularizer is a valid vectorial extension of TV and highlight connections with some other well-known vectorial TV extensions. 2) The derivation of an efficient optimization algorithm—based on duality principles—that is applicable to large volumes of data. 3) The illustration of our algorithm achieving better denoising performance than the existing vectorial TV and curl-divergence models. We further apply the framework to a real PC MRI data of blood flow in the human aorta.

II. Flow Field Regularization

We represent a flow field (d-dimensional vector field with d components) by the vector function $\mathbf{f}(\mathbf{x}) = (f_1(\mathbf{x}), \ldots, f_d(\mathbf{x}))$

Manuscript received August 12, 2014; revised November 05, 2014; accepted November 07, 2014. Date of publication November 10, 2014; date of current version November 19, 2014. This work was supported by the Center for Biomedical Imaging of the Geneva-Lausanne Universities and EPFL, and by the European Commission under Grant ERC-2010-AdG 267439-FUN-SP, and by the Swiss National Science Foundation (SNF) under Grant P300P2_151325. The associate editor coordinating the review of thi smanuscript and approving it for publication was Prof. Mehdi Moradi.

E. Bostan and M. Unser are with the Biomedical Imaging Group, School of Engineering, Laboratoire d'imagerie biomédicale, École polytechnique fédérale de Lausanne (EPFL), Lausanne CH-1015, Switzerland. (e-mail: emrah.bostan@epfl.ch; michael.unser@epfl.ch).

S. Lefkimmiatis is with the Department of Mathematics, University of California, Los Angeles (UCLA), Los Angeles, CA 90095 USA (e-mail: stamatis@math.ucla.edu).

O. Vardoulis and N. Stergiopulos are with the Laboratory of Hemodynamics and Cardiovascular Technology, Institute of Bioengineering, École polytechnique fédérale de Lausanne (EPFL) de Lausanne (EPFL), Lausanne CH-1015, Switzerland (e-mail: nikolaos.stergiopulos@epfl.ch; orestis.vardoulis@epfl.ch).

Color versions of one or more of the figures in this paper are available online at http://ieeexplore.ieee.org.

Digital Object Identifier 10.1109/LSP.2014.2369212

1070-9908 © 2014 IEEE. Personal use is permitted, but republication/redistribution requires IEEE permission.
See http://www.ieee.org/publications_standards/publications/rights/index.html for more information.

over $\mathbb{R}^d$ and consider the generic regularized least-squares problem:

$$\mathbf{f}^\star = \arg\min_{\mathbf{f}} \frac{1}{2}\|\mathbf{y}-\mathbf{f}\|_2^2 + \tau\mathcal{R}(\mathbf{f}). \tag{1}$$

In (1), $\mathbf{y}$ is the noisy flow while $\mathcal{R}$ is the regularizer that imposes certain characteristics on $\mathbf{f}^\star$. The parameter $\tau > 0$ controls the strength of regularization. We note that (1) is well-suited for Gaussian noise and can be modified for different noise models [12]. Next, we review some existing regularization methods.

As mentioned in Section I, curl-divergence regularization is commonly used for the reconstruction task. Fundamentally, the irrotational and incompressible characteristics of fluid flows are governed by these operators. As a regularizer, they are combined together in the following form:

$$\mathrm{CD}(\mathbf{f}) = \tau_c\|\mathbf{curl}\,\mathbf{f}\|_1 + \tau_d\|\mathrm{div}\,\mathbf{f}\|_1, \tag{2}$$

where $\|\cdot\|_1$ denotes (both scalar and vector) L_1-norms[1]. We refer the reader to [3] for further details regarding the treatment of $\mathbf{curl}$ and div operators in d-dimensions.

Total variation (TV) is among the most popular regularizers for imaging applications [13]. TV is applicable to scalar fields, $f : \mathbb{R}^d \mapsto \mathbb{R}$, and is defined as

$$\mathrm{TV}(f) = \int_{\mathbb{R}^d} \|\nabla f(\mathbf{x})\|_2 \mathrm{d}\mathbf{x}. \tag{3}$$

TV does not over penalize high variations of f so that it preserves intensity discontinuities. Due to this favorable property, TV has been extended to vector fields with the main requirement being that the vectorial variants should coincide with the definition of the scalar one (3) for $d = 1$.

The most simple and straightforward extension of TV involves the penalization of the intensity variation of every component of the vector field in a separable way. This leads to the following definition of the *separable* TV [14]:

$$\mathrm{TV}_S(\mathbf{f}) = \sum_{i=1}^{d} \int_{\mathbb{R}^d} \|\nabla f_i(\mathbf{x})\|_2 \mathrm{d}\mathbf{x}. \tag{4}$$

While (4) is easy to work with, one potential problem is that it does not take into account the dependencies (whether they are physical or not) that might exist among the different components of the vector data. For this reason, alternative extensions that provide a coupling between the components have also been studied. Among them, the most popular one is the *vectorial total variation* (VTV) [9] which is defined as

$$\mathrm{VTV}(\mathbf{f}) = \int_{\mathbb{R}^d} \left(\sum_{i=1}^{d} \|\nabla f_i(\mathbf{x})\|_2^2\right)^{1/2} \mathrm{d}\mathbf{x}. \tag{5}$$

A. Nuclear Total Variation

In this work, we propose to solve the flow field denoising problem in (1) by using an alternative vectorial extension of TV, termed as *nuclear total variation*, (TVN). As we shall show experimentally, the TVN regularizer can model the dependencies between the flow field components more efficiently than the existing vectorial TV extensions and, thus, it leads to improved denoising results.

To motivate the definition of TVN, we first need to establish a connection with the standard TV functional. The main component of TV is the gradient magnitude which is essentially capturing the intensity variations that are being penalized. As for the flow field case, the natural extension of the gradient is the Jacobian operator defined as $\mathbf{Jf} = [\nabla f_1 \ldots \nabla f_d]^{\mathrm{T}}$. The Jacobian evaluated at a spatial location $\mathbf{x}$ corresponds to a matrix of size $d \times d$ that embodies all possible first-order information at that specific point. The information about the strength of the flow field variation is encoded in its d singular values while the directions of these variations are encoded in the corresponding singular vectors. This implies that a vectorial extension of TV should penalize the singular values of the Jacobian. One way to accomplish this is to define a generic regularizer of the form

$$\mathrm{TV}_p(\mathbf{f}) = \int_{\mathbb{R}^d} \|\mathbf{Jf}(\mathbf{x})\|_{\mathcal{S}_p} \mathrm{d}\mathbf{x}, \quad \forall p \geq 1 \tag{6}$$

where $\|\cdot\|_{\mathcal{S}_p}$ is the Schatten p-norm of a matrix [15]. This norm corresponds to computing the ℓ_p-norm of the singular values of the matrix argument. We note that in the case of a scalar field the Jacobian reduces to the gradient and the ℓ_p norm (for any $p \geq 1$) of its singular value is equal to the gradient magnitude. Therefore, all the regularizers of the form (6) are valid vectorial TV extensions. In fact, the two existing vectorial extensions of TV that couple the components of the field can be directly obtained from the above definition. Specifically, for $p = 2$, we recover the *vectorial total variation* (VTV) [9]

$$\mathrm{TV}_2(\mathbf{f}) = \int_{\mathbb{R}^d} \|\mathbf{Jf}(\mathbf{x})\|_F \mathrm{d}\mathbf{x} = \mathrm{VTV}(\mathbf{f}), \tag{7}$$

where $\|\cdot\|_F$ is the Frobenius norm, while for $p = \infty$, we obtain the so-called "natural vectorial TV" of [10] defined as

$$\mathrm{TV}_\infty(\mathbf{f}) = \int_{\mathbb{R}^d} \|\mathbf{Jf}(\mathbf{x})\|_S \mathrm{d}\mathbf{x} = \mathrm{TVJ}(\mathbf{f}), \tag{8}$$

with $\|\cdot\|_S$ being the spectral (or the operator) norm.

Algorithm 1 TVN Reconstruction

1: **input:** $\mathbf{y}, \tau > 0$
2: **initalization:** $\psi_1 = \boldsymbol{\xi}_0 = \mathbf{0} \in \mathcal{X}, t_1 = 1$
3: **output:** $\mathbf{f}^\star$–Denoised flow field.
4: **repeat**
5: $\boldsymbol{\xi}_n \leftarrow \Pi_S(\psi_n + \frac{1}{12\tau}\mathbf{J}(\mathbf{y} - \tau\mathbf{J}^*\psi_n))$
6: $t_{n+1} \leftarrow \frac{1+\sqrt{1+4t_n^2}}{2}$
7: $\psi_{n+1} \leftarrow \boldsymbol{\xi}_n + (\frac{t_n-1}{t_{n+1}})(\boldsymbol{\xi}_n - \boldsymbol{\xi}_{n-1})$
8: $n \leftarrow n+1$
9: **until** stopping criterion
10: **return** $(\mathbf{y} - \tau\mathbf{J}^*\boldsymbol{\xi}_{n-1})$

[1]Vector L_1-norms are defined as the scalar L_1-norm of the magnitude of the vector field.

Based on the above discussion, it is further possible to derive another vectorial extension of TV by choosing $p = 1$. In this case, we have

$$\mathrm{TV}_1 = \int_{\mathbb{R}^d} \|\mathbf{J}\mathbf{f}(\mathbf{x})\|_N \mathrm{d}\mathbf{x} = \mathrm{TVN}(\mathbf{f}), \tag{9}$$

where $\|\cdot\|_N$ is the nuclear norm. From definition (9), we observe that TVN introduces a coupling between the flow field components by imposing an ℓ_1-penalty on the singular values of the Jacobian. In other words, TVN promotes flow field reconstructions where the Jacobian at each spatial location is approximately of low-rank[2]. Therefore, it preserves the variation at the dominant orientation (expectedly the flow itself), as the small variations (introduced by noise) are reduced. We note that TVN can be interpreted as a special case of the regularization family that we recently introduced in [11], which penalizes the rooted eigenvalues of the structure tensor of an image. Finally, we show that the TV_p regularizers satisfy the following invariance properties[3], which are essential for any regularizer applied on flow fields (see [3] for a detailed discussion).

Proposition 1: The regularizer TV_p, defined as in (6), is invariant under translation, scaling (up to a multiplicative factor), and rotation, where the rotation of a flow field $\mathbf{f}$ by some orthogonal matrix ξ is given by $\mathbf{f} \mapsto \xi^{\mathrm{T}}\mathbf{f}(\xi\,\cdot)$.

III. Reconstruction Algorithm

In the sequel, we consider the discrete version of TVN and describe a fast algorithm for solving (1). Specifically, we obtain the denoised flow field as the minimizer of the following strictly convex energy functional

$$\mathbf{f}^\star = \arg\min_{\mathbf{f}} \frac{1}{2}\|\mathbf{y}-\mathbf{f}\|_2^2 + \tau\|\mathbf{J}\mathbf{f}\|_{1,N}, \tag{10}$$

where $\mathbf{f}$ has been vectorized and is of size $\mathbb{R}^{k\cdot d}$, with k denoting the cardinality of the discrete index set (*e.g.* the number of voxels in 3-D). Further, $\|\mathbf{J}\mathbf{f}\|_{1,N} = \sum_{j=1}^{k}\|(\mathbf{J}\mathbf{f})_j\|_N$ is a compact notation for the discrete TVN that employs the mixed ℓ_1-nuclear norm and the discrete Jacobian $\mathbf{J} : \mathbb{R}^{k\cdot d} \mapsto \mathbb{R}^{k\times d\times d} \triangleq \mathcal{X}$. Invoking [16, Lemma 1] and considering Legendre-Fenchel duality [17], we derive the following dual definition for the discrete TVN:

$$\begin{aligned}\mathrm{TVN}(\mathbf{f}) &= \max_{\boldsymbol{\xi}\in\mathcal{X},\boldsymbol{\xi}_j\in\mathcal{B}_S^{d\times d}} \sum_{i=1}^{d}\sum_{j=1}^{k}(f_i)_j\nabla^*(\boldsymbol{\xi}_i)_j \\ &= \langle \mathbf{f}, \mathbf{J}^*\boldsymbol{\xi}\rangle_{\mathcal{X}}\end{aligned} \tag{11}$$

where ∇^* and $\mathbf{J}^*$ are the adjoints of the discrete gradient and Jacobian, respectively. In (11), $\boldsymbol{\xi} = (\boldsymbol{\xi}_1,\ldots,\boldsymbol{\xi}_k) \in \mathcal{X}$ is a dual variable with $(\boldsymbol{\xi}_i)_j$ referring to the ith row of the matrix $\boldsymbol{\xi}_\mathbf{j} \in \mathbb{R}^{d\times d}$, while $\mathcal{B}_S^{d\times d} = \{\mathbf{A}\in\mathbb{R}^{d\times d} : \|\mathbf{A}\|_S \le 1\}$ is the spectral unit-norm ball. Using the min-max theorem, we rewrite (10) in the equivalent form

$$\max_{\boldsymbol{\xi}\in\mathcal{X},\boldsymbol{\xi}_j\in\mathcal{B}_S^{d\times d}} \min_{\mathbf{f}} \frac{1}{2}\left(\|\mathbf{f}-\mathbf{u}\|_2^2 + \|\mathbf{y}\|_2^2\right) - \|\mathbf{u}\|_2^2 \tag{12}$$

where $\mathbf{u} = (\mathbf{y} - \tau\mathbf{J}^*\boldsymbol{\xi})$. Based on this development, the solution is derived in closed form as $\mathbf{f}^\star = (\mathbf{y} - \tau\mathbf{J}^*\boldsymbol{\xi}^\star)$, where $\boldsymbol{\xi}^\star$ corresponds to the maximizer

$$\boldsymbol{\xi}^\star = \operatorname*{argmax}_{\boldsymbol{\xi}\in\mathcal{X},\boldsymbol{\xi}_j\in\mathcal{B}_S^{d\times d}} \|\mathbf{y}\|_2^2 - \|\mathbf{y}-\tau\mathbf{J}^*\boldsymbol{\xi}\|_2^2\,. \tag{13}$$

Since the function in (13) is smooth with well-defined gradient we compute $\boldsymbol{\xi}^\star$ using an accelerated projected gradient ascent based on Nesterov's method [18]. The details of the approach are given in Algorithm 1. We note that in Algorithm 1 the operation Π_S refers to the indepckendent projection of each of the k matrices onto the $\mathcal{B}_S^{d\times d}$ unit ball. To perform this operation, we rely on the result of [16, Proposition 1] which provides a connection between matrix and vector projections. For a matrix $\mathbf{X}$ with singular value decomposition $\mathrm{SVD}(\mathbf{X}) = \mathbf{USV}$, the projection is performed as $\Pi_S(\mathbf{x}) = \mathbf{XVS}^+\tilde{\mathbf{S}}\mathbf{V}^{\mathrm{T}}$. Here, $\mathbf{S}^+$ is the pseudo-inverse of $\mathbf{S}$ and $\tilde{\mathbf{S}}$ is the diagonal matrix which contains the projected singular values of $\mathbf{S}$ onto the ℓ_∞ unit-norm ball. This projection sets to one the singular values that exceed this value while leaving the rest untouched. It is noteworthy that SVD can be performed very efficiently for 3D flow fields.

IV. Experimental Results

Based on the above developments, we now conduct experiments in simulated and practical configurations, where all visualizations are generated with ParaView (Kitware Inc.).

We first consider the problem of recovering a volumetric ($d = 3$) flow field from noisy measurements and compare the reconstruction performance of the following methods: 1) CD regularization given in (2), 2) TV_S regularization given in (4), 3) VTV regularization given in (5), 4) TVJ regularization given in (8), and 5) Our method TVN given in (9).

We generate a dataset composed of four different three-dimensional phantom models (see Fig. 1). The measurements are obtained by degrading the data with different levels of additive white Gaussian noise. For all methods, we use the same optimization algorithm that combines the duality arguments with Nesterov's method [18]. Note that this algorithm has been developed in [19] for CD, and in [10], [20], [21] for the existing vectorial extensions of TV. In all cases, the stopping criterion is set to either reaching a relative ℓ_2-normed difference of 10^{-4} between two successive estimates, or a maximum of 500 iterations. For each regularization method, the regularization parameter is optimized for the best-possible SNR performance using an oracle.

By inspecting the results given in Table I, we see that the TVN outperforms CD and the vectorial TV methods for most of the simulated fields considered in the experiments. This demonstrates the ability of our regularization scheme to preserve the rapid changes at the boundaries (see Fig. 2). One surprising result provided by the experiments is that the performance of TV_S is highly competitive. Even though, this model simply does not capture the vectorial nature of the flow data, it achieves the best performance for the Tube phantom. This is explained by the fact that Tube is a separable phantom (superposition of 2D flow fields) by construction.

As a supplement to our *in silico* experiments, we now consider a volumetric PC MRI dataset in the aortic arch region of a young, healthy, male volunteer. PC MRI data was acquired with a sagittal oblique 3D slab covering the entire aortic arch, using

[2]The nuclear norm is the convex envelope of the rank of a matrix.

[3]Proof is available at http://bigwww.epfl.ch/publications/bostan1501doc01.pdf

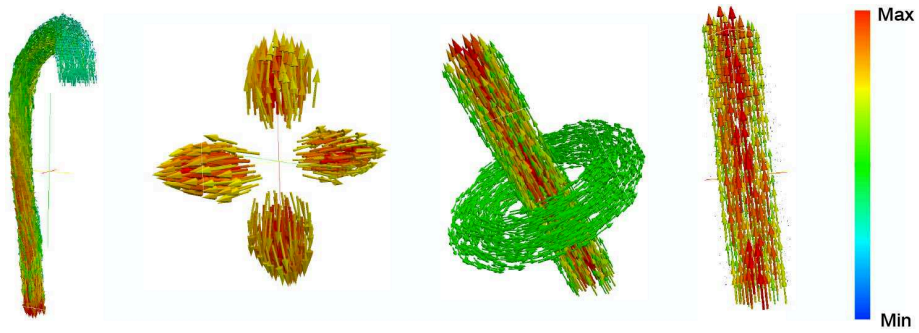

Fig. 1. Illustration of the flow fields used in the experiments: From left to right, they are called 1) Blood flow, 2) Gradient, 3) Torus, and 4) Tube.

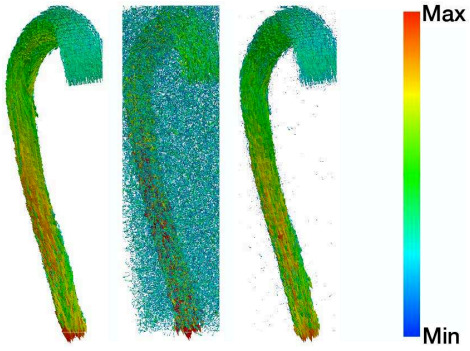

Fig. 2. Denoising of the simulated blood flow: original flow (left), noisy flow (middle, $\mathrm{SNR} = 0$ dB), and the denoised flow (right, $\mathrm{SNR} = 16.55$ dB) by using the proposed method.

TABLE I
RESULTS OF THE DENOISING EXPERIMENTS ON SIMULATED DATA

		Reconstruction SNR [dB]				
	SNR [dB]	CD	TV_S	VTV	TVJ	TVN
Tube	0	14.47	**19.66**	17.64	16.42	19.19
	10	22.67	**27.09**	24.62	23.37	26.47
	20	30.72	**34.89**	31.96	30.75	34.20
	30	39.29	**43.38**	40.09	39.05	42.89
Torus	0	13.49	17.59	16.25	14.63	**18.07**
	10	20.37	25.30	23.63	22.24	**26.08**
	20	29.17	33.66	31.78	30.48	**34.63**
	30	38.28	42.34	40.40	39.42	**43.60**
Gradient	0	15.19	19.51	19.64	18.43	**20.77**
	10	23.24	26.82	27.72	26.81	**28.39**
	20	31.86	35.30	36.54	35.77	**36.80**
	30	41.07	44.40	45.73	45.03	**45.89**
Blood	0	12.70	15.80	15.33	13.86	**16.55**
	10	19.34	22.44	22.43	21.35	**23.45**
	20	27.44	29.92	30.35	29.62	**30.92**
	30	36.37	38.42	39.01	38.44	**39.24**

a navigator-gated, ECG-gated RF-spoiled gradient echo (GRE) sequence [22]. The scan was performed at a 3T clinical MR scanner (MAGNETOM Trio, Siemens AG, Healthcare Sector, Erlangen, Germany). The sequence was motion compensated.

To regularize the data, we assess for the time point of peak ascending aortic flow. We use TVN with 250 iterations where we manually calibrate the regularization parameter. Streamlines are generated for both pre- and post-regularization states by using identical number of seed points, seed area and integration length.

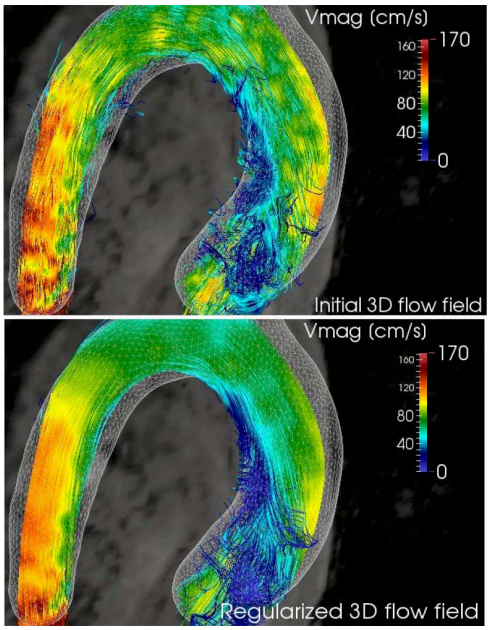

Fig. 3. Enhancement of streamline visualizations of a real phase-contrast MRI recording: Original aortic blood flow data in the aortic arch (top) and the data after processing with the proposed method (bottom). See text for further details of the experiment.

A qualitative examination of Fig. 3 shows that the amount of streamline artifacts is decreased especially in the ventral side of the arch. We also observe that the rapid velocity changes in the flow (at both the ascending and descending aorta) are reduced. The latter can be useful for estimating the first order velocity derivatives that are required for important physical parameters such as vorticity and flow helicity [22], [23]. These aspects suggest that our method is beneficial for the visualization of aortic hemodynamic phenomena.

V. CONCLUSION

We considered the problem of flow field denoising and employed a regularizer that penalizes the nuclear norm of the Jacobian of the field. We first conducted denoising experiments on different phantom data involving rapid transitions at the flow boundaries. We observed that the proposed method yielded better SNR performance (up to 1.3 dB) than the curl-divergence regularizers and the existing vectorial extensions of total variation. We also used our reconstruction algorithm for enhancing streamline visualizations of a real phase-contrast MRI recording.

REFERENCES

[1] J. G. Santiago, S. T. Wereley, C. D. Meinhart, D. J. Beebe, and R. J. Adrian, "A particle image velocimetry system for microfluidics," *Exper. Fluids*, vol. 25, no. 4, pp. 316–319, 1998.

[2] M. Markl, A. Frydrychowicz, S. Kozerke, M. Hope, and O. Wieben, "4D flow MRI," *J. Magn. Reson. Imag/*, vol. 36, no. 5, pp. 1015–1036, 2012.

[3] P. D. Tafti and M. Unser, "On regularized reconstruction of vector fields," *IEEE Trans. Image Process.*, vol. 20, no. 11, pp. 3163–3178, 2011.

[4] P. D. Tafti, R. Delgado-Gonzalo, A. F. Stalder, and M. Unser, "Variational enhancement and denoising of flow field images," in *Proc. the 8th IEEE Int. Symp. Biomedical Imaging: From Nano to Macro (ISBI'11)*, Chicago, IL, USA, Mar., Apr. 30, 2, 2011, pp. 1061–1064.

[5] E. Bostan, O. Vardoulis, D. Piccini, P. D. Tafti, N. Stergiopulos, and M. Unser, "Spatio-temporal regularization of flow-fields," in *Proc. 10th IEEE Int. Symp. Biomedical Imaging: From Nano to Macro (ISBI'13)*, San Francisco, CA, USA, Apr. 7–11, 2013, pp. 836–839.

[6] S. N. Gupta and J. L. Prince, "On div-curl regularization for motion estimation in 3-d volumetric imaging," in *Proc. 3rd IEEE Int. Conf. Image Processing (ICIP'96)*, Lausanne, Switzerland, Sep. 16–19, 1996, vol. 1, pp. 929–932.

[7] D. Suter and F. Chen, "Left ventricular motion reconstruction based on elastic vector splines," *IEEE Trans. Med. Imag.*, vol. 19, no. 4, pp. 295–305, 2000.

[8] M. Arigovindan, M. Sühling, C. Jansen, P. Hunziker, and M. Unser, "Full motion and flow field recovery from echo doppler data," *IEEE Trans. Med. Imag.*, vol. 26, no. 1, pp. 31–45, 2007.

[9] P. Blomgren and T. F. Chan, "Color TV: Total variation methods for restoration of vector-valued images," *IEEE Trans. Image Process.*, vol. 7, no. 3, pp. 304–309, 1998.

[10] B. Goldluecke, E. Strekalovskiy, and D. Cremers, "The natural vectorial total variation which arises from geometric measure theory," *SIAM J. Imag. Sci.*, vol. 5, no. 2, pp. 537–563, 2012.

[11] S. Lefkimmiatis, A. Roussos, M. Unser, and P. Maragos, "Convex generalizations of total variation based on the structure tensor with applications to inverse problems," *Scale Space Variational Meth. Comput. Vis.*, vol. 7893, pp. 48–60, 2013.

[12] F.-X. Dupé, J. Fadili, and J.-L. Starck, "Linear inverse problems with various noise models and mixed regularizations," in *Proc. 5th Int. ICST Conf. Performance Evaluation Methodologies and Tools (VALUETOOLS '11)*, Brussels, Belgium, 2011, pp. 621–626.

[13] L. Rudin, S. Osher, and E. Fatemi, "Nonlinear total variation based noise removal algorithms," *Physica D*, vol. 60, pp. 259–268, 1992.

[14] H. Attouch, G. Buttazzo, and G. Michaille, *Variational Analysis in Sobolev and BV Spaces: Applications to PDEs and Optimization*, ser. MPS-SIAM Series on Optimization. Philadelphia, PA, USA: SIAM, 2006.

[15] R. Bhatia, *Matrix Analysis*. Berlin, Germany: Springer, 1997.

[16] S. Lefkimmiatis, J. Ward, and M. Unser, "Hessian Schatten-norm regularization for linear inverse problems," *IEEE Trans. Image Process.*, vol. 22, no. 5, pp. 1873–1888, 2013.

[17] S. Boyd and L. Vandenberghe, *Convex Optimization*. New York, NY, USA: Cambridge Univ. Press, 2004.

[18] Y. Nesterov, "A method of solving a convex programming problem with convergence rate $O(1/k^2)$," *Sov. Math. Doklady*, vol. 27, no. 2, pp. 372–376, 1983.

[19] E. Bostan, P. D. Tafti, and M. Unser, "A dual algorithm for L_1-regularized reconstruction of vector fields," in *Proc. 9th IEEE Int. Symp. Biomedical Imaging: From Nano to Macro (ISBI'12)*, Barcelona, Spain, May 2–5, 2012, pp. 1579–1582.

[20] A. Beck and M. Teboulle, "Fast gradient-based algorithms for constrained total variation image denoising and deblurring problems," *IEEE Trans. Image Process.*, vol. 18, no. 11, pp. 2419–2434, 2009.

[21] X. Bresson and T. F. Chan, "Fast dual minimization of the vectorial total variation norm and applications to color image processing," *Inv. Probl. Imag.*, vol. 2, no. 4, pp. 455–484, 2008.

[22] M. Markl, P. Kilner, and T. Ebbers, "Comprehensive 4D velocity mapping of the heart and great vessels by cardiovascular magnetic resonance," *J. Cardiovasc. Magn. Res.*, vol. 13, no. 1, pp. 7–, 2011.

[23] U. Morbiducci, R. Ponzini, G. Rizzo, M. Cadioli, A. Esposito, F. D. Cobelli, A. D. Maschio, F. M. Montevecchi, and A. Redaelli, "In vivo quantification of helical blood flow in human aorta by time-resolved three-dimensional cine phase contrast magnetic resonance imaging," *Ann. Biomed. Eng.*, vol. 37, no. 3, pp. 516–531, 2009.